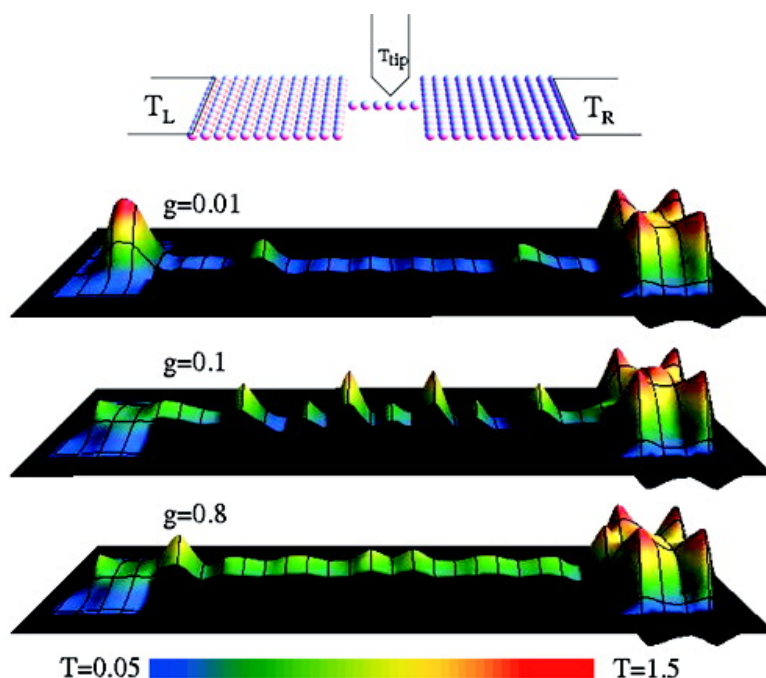


## Thermoelectric Effects in Nanoscale Junctions

Yonatan Dubi, and Massimiliano Di Ventra

*Nano Lett.*, **2009**, 9 (1), 97-101 • DOI: 10.1021/nl8025407 • Publication Date (Web): 10 December 2008

Downloaded from <http://pubs.acs.org> on January 14, 2009



### More About This Article

Additional resources and features associated with this article are available within the HTML version:

- Supporting Information
- Access to high resolution figures
- Links to articles and content related to this article
- Copyright permission to reproduce figures and/or text from this article

[View the Full Text HTML](#)



ACS Publications  
High quality. High impact.

# Thermoelectric Effects in Nanoscale Junctions

Yonatan Dubi\* and Massimiliano Di Ventra

Department of Physics, University of California San Diego,  
La Jolla, California 92093-0319

Received August 20, 2008; Revised Manuscript Received November 24, 2008

## ABSTRACT

Despite its intrinsic nonequilibrium origin, thermoelectricity in nanoscale systems is usually described within a static scattering approach which disregards the dynamical interaction with the thermal baths that maintain energy flow. Using the theory of open quantum systems, we show instead that unexpected properties, such as a resonant structure and large sign sensitivity, emerge if the nonequilibrium nature of this problem is considered. Our approach also allows us to define and study a local temperature, which shows hot spots and oscillations along the system according to the coupling of the latter to the electrodes. This demonstrates that Fourier's law—a paradigm of statistical mechanics—is generally violated in nanoscale junctions.

**Introduction.** Nonequilibrium (NE) processes at the nanoscale are receiving a great deal of attention due in large part to the advancements in fabrication and manipulation of these systems.<sup>1</sup> An especially interesting class of NE phenomena pertains to energy transport and the conversion of thermal to electrical energy. When a thermal gradient  $\Delta T$  is applied to a finite system, electrons respond by departing from their ground state to partially accumulate at one end of the system, thus creating a measurable voltage difference  $\Delta V$ . The ratio  $S = -(\Delta V)/(\Delta T)$  is called thermopower<sup>2</sup> and has been measured in a variety of nanoscale systems such as quantum point contact,<sup>3</sup> atomic-size metallic wires,<sup>4</sup> quantum dots,<sup>5-7</sup> Si nanowires,<sup>8,9</sup> and recently in molecular junctions.<sup>10</sup> In bulk material, when  $S < 0$  the transient current is carried by electrons; when  $S > 0$  it is carried by holes.

In nanoscale systems this NE problem has recently received a lot of attention.<sup>3,12-22</sup> In these theories, the single-particle scattering formalism<sup>23-25</sup> is used to relate the thermopower to single-particle transmission probabilities. This approach, however, does not take into account the dynamical formation of the thermopower and neglects the fact that even at steady state, when the charge current is zero, an energy current is still present, like, e.g., in insulators.<sup>26</sup> Another effect neglected by such theories, which is now within reach of experimental verification,<sup>27</sup> is the formation of local temperature variations along the structure. In order to study all these effects, one needs to describe a nanoscale system interacting with an environment that maintains the thermal gradient, namely, one needs to resort to a theory of NE open quantum systems.

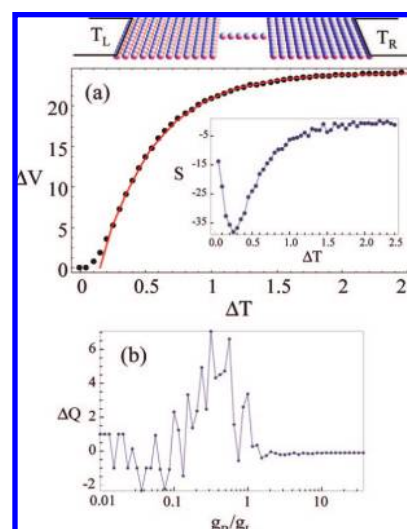


**Figure 1.** (a) Upper panel: nanojunction geometry considered in this calculation (see text for parameters). Main panel: Voltage drop  $\Delta V$  across the junction as a function of the temperature difference between the leads. There are three distinct regimes: a regime of vanishingly small response, a regime of rapid voltage rise, and saturation. The solid line is a fit to an exponential rise. Inset: generalized thermopower,  $S = -(d(\Delta V))/(d(\Delta T))$ . (b) Charge imbalance  $\Delta Q$  as a function of the ratio between the right and left lead-wire coupling  $g_R/g_L$ , at a constant  $g_L = 0.001$  and at  $\Delta T = 1$ .

In this Letter we introduce such a theory, based on a generalization of quantum master equations, and use it to study the dynamical formation of thermoelectric effects in nanojunctions. We show that the thermopower is a highly nonlinear function of the thermal gradient and it is very sensitive to the junction geometry, even in the simplest case

\* Corresponding author, dubij@physics.ucsd.edu.

of noninteracting electrons. This precludes an easy interpretation of its sign in terms of electrons or holes as it has been argued in some literature.<sup>3,12-17</sup> In addition, we calculate the global and local electron distribution functions, which exhibit NE characteristics.

The theory also allows us to define the local electron temperature by means of a *temperature floating probe* that is locally coupled to the system and whose temperature is adjusted so that the system dynamics is minimally perturbed. This temperature, which can be measured experimentally, shows interesting features such as hot spots in the cold lead at small coupling between the nanowire and the bulk electrodes and temperature oscillations in the wire at intermediate coupling. These findings show that Fourier's law, which is considered a paradigm of thermodynamics, is generally violated for electronic systems at the nanoscale.<sup>28</sup>

**Method.** Since we consider noninteracting electrons coupled to an environment, we employ a quantum master equation of the Lindblad type<sup>29</sup> which describes the dynamical evolution of the many-body density matrix (DM)  $\rho_M$  of a quantum system in the presence of a Markovian bath, via the introduction of a superoperator  $\mathcal{L}[\rho_M]$ .<sup>30</sup> The quantum master equation is then ( $\hbar = 1$ )

$$\dot{\rho}_M = -i[\mathcal{H}, \rho_M] + L[\rho_M] \quad (1)$$

where  $[\cdot, \cdot]$  denotes the commutator. The superoperator  $\mathcal{L}$  is defined via a set  $V_{nn'}$  of operators via

$$L[\rho_M] = \sum_{n,n'} \left( -\frac{1}{2} \{V_{nn'}^\dagger V_{nn'}, \rho_M\} + V_{nn'} \rho_M V_{nn'}^\dagger \right) \quad (2)$$

with  $\{\cdot, \cdot\}$  being the anticommutator. The sums over  $n$  and  $n'$  ( $n \neq n'$ ) are performed over all many-particle levels of the system, and the  $V$  operators are conveniently selected in the form  $V_{nn'} = (\gamma_{nn'})^{1/2} |\Psi_n\rangle \langle \Psi_{n'}|$ , describing a transition from the many-body state  $|\Psi_{n'}\rangle$  into the state  $|\Psi_n\rangle$  with the transition rate  $\gamma_{nn'}$ .

This problem scales exponentially with the number of particles, but recently a mapping of the many-body superoperator to a single-particle form has been introduced.<sup>31</sup> This results in a quantum master equation for the *single-particle* DM,  $\rho = \sum_{kk'} \rho_{kk'} |k\rangle \langle k'|$  which provides excellent agreement with the many-body solution. Here,  $|k\rangle$  represents the single-particle states, and the matrix elements are derived from the many-body DM by  $\rho_{kk'} = \text{Tr}(c_k^\dagger c_{k'} \rho_M)$ .

To be specific, we consider a finite nanojunction (i.e., with a fixed number of electrons and ions) which is composed of two identical quasi-two-dimensional leads connected via a one-dimensional wire (see upper panel of Figure 1). The far edges of the leads are coupled to two different baths kept at different temperatures. The Hamiltonian of the system is given by  $\mathcal{H} = \mathcal{H}_L + \mathcal{H}_R + \mathcal{H}_d + \mathcal{H}_c$ , where  $\mathcal{H}_{L,R,d} = -t \sum_{(i,j) \in L,R,d} (c_i^\dagger c_j + h.c.)$  are the tight-binding Hamiltonians of the left lead, right lead, and wire, respectively ( $t$  is the hopping integral, which serves as the energy scale hereafter), and  $\mathcal{H}_c = (g_{Lc} c_{d,0}^\dagger + g_{Rc} c_{d,L_d}^\dagger + h.c.)$  describes the coupling between the left (right) lead to the wire, with  $c_{L(R)}^\dagger$  being the creation operator for an electron at the point of contact between the left (right) lead and the wire, and  $c_{d,0}$  ( $c_{d,L_d}$ ) destroys an electron at the left-most (right-most) sites

of the wire. We consider here spinless electrons. The master equation now takes the form

$$\dot{\rho} = -i[\mathcal{H}, \rho] + L_L[\rho] + L_R[\rho] \quad (3)$$

where  $L_{L(R)}$  describes relaxation processes due to the contact between the left (right) lead with its respective bath at temperature  $T_{L(R)}$ . The  $V$  operators are generalized to account for the different baths and are given by<sup>31,32</sup>

$$V_{kk'}^{(L,R)} = \sqrt{\gamma_{kk'}^{(L,R)} f_D^{(L,R)}(\epsilon_k)} |k\rangle \langle k'| \quad (4)$$

where

$$f_D^{(L,R)}(\epsilon_k) = 1 / \left( \exp\left(\frac{\epsilon_k - \mu}{k_B T_{L,R}}\right) + 1 \right)$$

represents the Fermi distributions of the left and right leads, with  $\mu$  the chemical potential. The coefficients

$$\gamma_{kk'}^{(L,R)} = \left| \sum_{r_i \in S_{L(R)}} \psi_k(r_i) \gamma_0 \psi_{k'}^*(r_i) \right| \quad (5)$$

describe the overlap between the single-particle states  $|k\rangle$  and  $|k'\rangle$  over the region of contact  $S_{L(R)}$  between the left (right) baths and the corresponding junction leads, shown by the solid lines in the upper panel of Figure 1.  $\gamma_0$  describes the strength of electron-phonon (bath) interaction. The form (5) can be derived from first principles by tracing out the bath degrees of freedom, with the latter formed by a dense spectrum of boson excitations (e.g., phonons), which interact *locally* with electrons at the edges of the system. The operators (4) guarantee that the system evolves to a global equilibrium if  $T_L = T_R$  or equilibrate each lead at its own temperature if  $g = 0$ ; i.e., the leads and the wire are completely decoupled (and hence no voltage drop can form).

We now solve eq 3 numerically for several temperature gradients. From the obtained charge density distribution we derive the electrical potential via the Poisson equation. The potential is averaged along the transverse direction, and the voltage drop is calculated from the center of the leads.<sup>33</sup> The off-diagonal elements of the DM decay fast (on a time-scale  $\sim \gamma_0^{-1} \sim 10$  in our calculations) and hence do not contribute to the density in the long-time limit. This allows us to neglect them completely, a fact which significantly simplifies the calculation.<sup>34</sup>

**Numerical Results.** In Figure 1a the voltage drop  $\Delta V$  across the junction is plotted as a function of the temperature difference  $\Delta T$  between the contacts. The leads are of dimensions  $12 \times 11$  and the wire is of length  $L_d = 6$ . The lead-wire coupling is  $g_L = g_R = 0.001$  and the number of electrons is  $n_E = 90$ , which corresponds to  $1/3$  filling. The initial temperatures are set to  $T_L = T_R = 0.05$ . From Figure 1 one notices several regimes in the range of  $\Delta T$ . At very small  $\Delta T$ , there seems to be a negligible thermoelectric response. This is partly due to the fact that the energy flow is not enough to overcome a capacitive energy barrier formed by the junction. In this case, the energy difference only causes charge dipoles<sup>26</sup> to be formed at the junction.<sup>35</sup> This regime is followed by a rapid rise in  $\Delta V$ , eventually reaching a saturation at large  $\Delta T$ , due to the finite size of the system. The solid line is a fit to an exponential rise. Although the parameters of the exponential fit depend on sample parameters, we found that the exponential form is an excellent fit

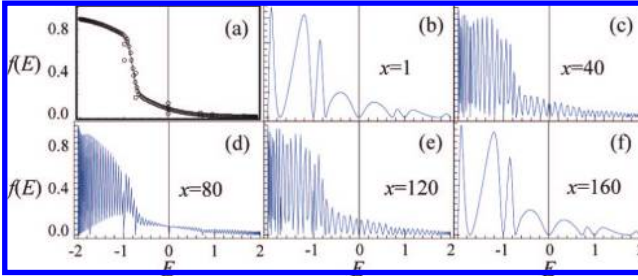


**Figure 2.** (a) Full distribution function of a long wire,  $L_d = 160$  (see text for numerical parameters). The solid line is a mean distribution function  $f(E) = \frac{1}{2}(f_D(T_L) + f_D(T_R))$ . (b–f) Local distribution function for different positions along the wire.

for all noninteracting junctions. In the inset of Figure 1a we plot the generalized thermopower

$$S = -\frac{d(\Delta V)}{d(\Delta T)}$$

which reduces to the regular thermopower in the linear regime. As seen,  $S$  exhibits a resonance at  $\Delta T \approx 0.25$  (this value is not universal and depends on junction parameters), which means that at this value the response of the system to a change in the temperature gradient is maximal; a fact that can be checked experimentally and may be used in actual devices.

**Geometrical Effects.** Due to the local variations of the density at the junction and hence local variations of kinetic energy, the thermoelectric response strongly depends on junction geometry, as it was anticipated experimentally.<sup>4</sup> As an example, we have calculated the charge imbalance,  $\Delta Q$ , across a junction (leads size  $6 \times 7$ , wire length  $L_d = 6$ , density at  $1/3$  filling) with an asymmetric coupling between the leads and the wire. The coupling to the left lead was kept at  $g_L = 0.001$  and the coupling to the right lead,  $g_R$ , was changed. In Figure 1b we plot the charge imbalance as a function of  $g_R$  at a fixed temperature difference  $\Delta T = 1$ . Strong and narrow oscillations can be seen, and for certain values of coupling asymmetry,  $\Delta Q$  may even change sign. This is consistent with the experiments in ref 4 and may account for the sign change of the thermopower observed in some experiments in molecular junctions.<sup>4,10,11</sup>

Let us give an estimate to the parameters in real junctions. In (semiconductor) quantum dots, the coupling between the leads and the dot is typically  $10^{-5}$  eV. In our units, that would correspond to a temperature of  $T_L \sim 6$  K, and a temperature difference of  $\Delta T \sim 30$  K for the maximum thermopower (inset of Figure 1). Saturation of  $\Delta V$  would thus occur at a temperature bias of  $\Delta T \sim 150$  K.

**Nonequilibrium Distributions.** The formalism presented here allows us to calculate various NE properties. As an example, we calculate the local and global distribution functions (DF) of the wire (which are accessible experimentally),<sup>36</sup> for a system with lead size  $5 \times 5$ , wire length  $L_d = 160$  (at third filling), with coupling  $g_L = g_R = 1$ , and temperatures  $T_L = 0.05$  and  $T_R = 0.5$ . In Figure 2a we plot the full distribution function of the wire (circles),  $f(E_k) = \rho_{kk}$ , along with the curve

$$f(E_k) = \frac{1}{2}(f_D(T_L) + f_D(T_R))$$

(solid line). As seen, the fit between the data and the DF is excellent. In Figure 2, panels b–f, we plot the local DF  $f(E_k, x) = \rho_{kk} |\psi_k(x)|^2$  for different positions along the wire,  $x = 1, 40, 80, 120, 160$  (respectively). Note the fast oscillations upon approaching the center of the wire and the symmetry with respect to the wire center. The origin of the oscillations lies both in the NE nature of the system and in the geometry (i.e., the fact that the wire is ballistic and that the wire-lead coupling is large). The systems of interest are finite and hence the wave function solutions are standing waves. Since the local distributions are proportional to the modulus of the wave function, they oscillate according to the oscillations of the wave functions.<sup>37</sup> In a system with small wire-lead coupling we found (not shown) that the oscillations persist at the center of the wire but are smoothed at the wire edges. Figure 2, panels b–f, shows that although the full DF is a simple average of the left and right lead distributions, one cannot assign a simple position dependence, as in the case of mesoscopic wires.<sup>36</sup>

**Local Temperature.** The concept of a local temperature is generally not unique out of equilibrium.<sup>38,39</sup> Here we provide an operational definition, which is both physically transparent and can (in principle) be directly probed experimentally.<sup>27</sup> In order to do so, we add an additional relaxation operator  $\mathcal{L}_{\text{tip}}[\rho_M]$  to the master equation (1). This corresponds to applying a local bath at a temperature  $T_{\text{tip}}$  in contact with a single site of the system (see upper panel of Figure 3). Due to energy flow between the probe and the coupled site, the system dynamics is generally modified. However, one can “float” the temperature  $T_{\text{tip}}$  such that the change in local (and hence global, e.g., thermopower) properties of the system is minimal. We define this temperature as the *local temperature* of our system at the probe position. We choose to monitor the change in the local density from its value in the absence of the probe but any other quantity would be equally valid and lead to the same local temperature.

Knowledge of the local temperature allows us to address the problem of validity of Fourier’s law at the nanoscale. It has been conjectured<sup>28</sup> and demonstrated for systems such as spin-chains<sup>32,40</sup> and coupled harmonic oscillators<sup>41,42</sup> that in ballistic quantum systems Fourier’s law is invalid. Stimulated by this unsolved problem, we plot in Figure 3 the local temperature at steady state for three different values of the lead-wire coupling,  $g = 0.001, 0.1, 0.8$  and a junction with lead dimensions  $4 \times 3$ , wire length  $L_d = 21$ , temperatures  $T_L = 0.05$  and  $T_R = 1.5$ , and electron density at third filling. For weak coupling ( $g = 0.001$ ), we find that the temperature inside the wire is very low, but a “hot spot” develops in the cold lead. As the coupling increases the hot spot vanishes, and temperature oscillations develop in the wire. As expected, at high coupling, the wire equilibrates at a temperature that is roughly the average between  $T_L$  and  $T_R$ . For large lead-wire coupling the temperature in the wire is uniform, and most of the temperature drop occurs at the contacts, similar to what has been argued for the phenomenon of local ionic heating.<sup>43</sup> Our results thus verify that Fourier’s law is generally violated in nanoscale junctions.

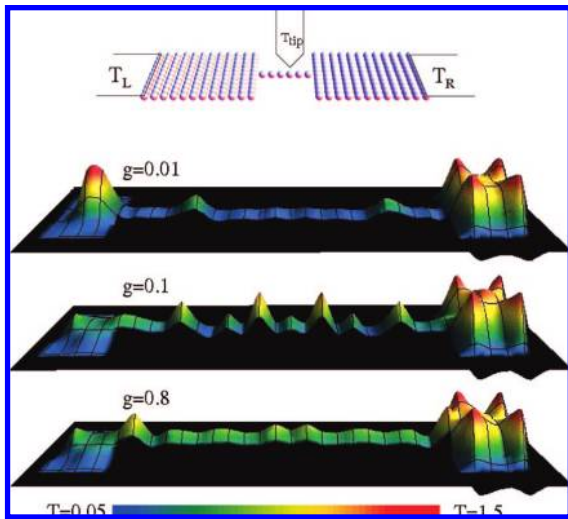


**Figure 3.** Upper panel: schematic representation of the calculation to determine the local temperature via the addition of a local temperature floating probe. Lower panels: the local temperature along the structure for three different values of the lead-wire coupling,  $g = 0.001, 0.1, 0.8$ . Three effects are observed: a hot-spot in the cold lead at small coupling, temperature oscillations in the wire at intermediate coupling, and uniform temperature along the wire at large coupling. All three constitute violations of Fourier's law.

In additional numerical results with longer wires and various wire-lead couplings, we found that the oscillations in the temperature strongly depend on the coupling, and the oscillation wavelength may vary between one lattice constant and up to tens of lattice constants. However, in typical molecular or metallic wires, these length scales are of nanometer scale and, therefore, are still beyond the resolution of present experiments that measure local temperatures.<sup>27,44</sup>

We also note that when the coupling  $g \sim 1$ , so that the wave functions are completely delocalized along the nano-junction, the thermopower is small. This is consistent with the experimental results of ref 4 where junctions of large conductance show small thermopower values.

**Summary.** We have shown, using an open quantum system approach, that the proper description of energy flow in nanoscale systems leads to unexpected features in the dynamical formation of thermopower. Several predictions have been made which can be tested experimentally, namely, (i) the nonlinear dependence (with resonant structures) of the thermopower as a function of the temperature gradient, (ii) its strong sensitivity (including sign) to junction geometry, (iii) the shape of the NE electron distribution at steady state, and (iv) we have provided an operational definition of local temperature as that measured by a temperature floating probe, i.e., one that is locally coupled to the system, and whose temperature is adjusted so that the system dynamics is minimally perturbed. This temperature shows noteworthy features according to the strength of the coupling between the nanoscale system and the electrodes, in violation of Fourier's law.

We conclude by pointing out that the results presented here may be relevant to other systems of present interest (e.g., graphene nanoribbons, nanotubes, etc.). Studies of these

effects that include electron interactions represent another important research direction and are underway using stochastic time-dependent current density-functional theory.<sup>45,46</sup>

**Acknowledgment.** We thank R. D'Agosta for useful discussions and DOE for support under Grant DE-FG02-05ER46204.

## References

- (1) For a review see, e.g.: Gaspard, P. *Prog. Theor. Phys. Suppl.* **2006**, *165*, 33.
- (2) See, e.g.: Pollock, D. D. *Thermoelectricity: Theory, Thermometry, Tool*; American Society for Testing and Materials: Philadelphia, PA, 1985.
- (3) van Houten, H.; Molenkamp, L. W.; Beenakker, C. W. J.; Foxon, C. T. *Semicond. Sci. Technol.* **1992**, *7*, B215.
- (4) Ludoph, B.; Ruitenbeek, J. M. *Phys. Rev. B* **1999**, *59*, 12290.
- (5) Staring, A. A. M.; Molenkamp, L. W.; Alphenaar, B. W.; van Houten, H.; Buyk, O. J. A.; Mabeoone, M. A. A.; Beenakker, C. W. J.; Foxon, C. T. *Europhys. Lett.* **1993**, *22*, 57.
- (6) Molenkamp, L.; Staring, A. A. M.; Alphenaar, B. W.; van Houten, H.; Beenakker, C. W. J. *Semicond. Sci. Technol.* **1994**, *9*, 903.
- (7) Godijn, S. F.; M. L. W.; van Langen, S. A. *Phys. Rev. Lett.* **1999**, *82*, 2927.
- (8) Hochbaum, A. I.; Chen, R.; Delgado, R. D.; Liang, W.; Garnett, E. C.; Najarian, M.; Majumdar, A.; Yang, P. *Nature* **2008**, *451*, 163.
- (9) Boukai, A. I.; Bunimovich, Y.; Tahir-Kheli, J.; Yu, J.-K.; Goddard, W. A., III; Heath, J. R. *Nature* **2008**, *451*, 168.
- (10) Reddy, P.; Jang, S.-Y.; Segalman, R. A.; Majumdar, A. *Science* **2007**, *315*, 1568.
- (11) Baheti, K.; Malen, J. A.; Doak, P.; Reddy, P.; Jang, S.-Y.; Tilley, T. D.; Majumdar, A.; Segalman, R. A. *Nano Lett.* **2008**, *8*, 715.
- (12) Paulsson, M.; Datta, S. *Phys. Rev. B* **2003**, *67*, 241403(R)
- (13) Lunde, A. M.; Flensberg, K. *J. Phys.: Condens. Matter* **2005**, *17*, 3879.
- (14) Lunde, A. M.; Flensberg, K. J.; Glazman, L. I. *Phys. Rev. Lett.* **2005**, *97*, 256802.
- (15) Beenakker, C. W. J.; Starling, A. A. M. *Phys. Rev. B* **1992**, *46*, 9667.
- (16) Koch, J.; Von Oppen, F.; Oreg, Y.; Sela, E. *Phys. Rev. B* **2004**, *70*, 195107.
- (17) Segal, D. *Phys. Rev. B* **2005**, *72*, 165426.
- (18) Pauly, F.; Viljas, J. K.; Cuevas, J. C. *Phys. Rev. B* **2008**, *78*, 035315.
- (19) Freericks, J. K.; Zlatić, V.; Shvaika, A. M. *Phys. Rev. B* **2007**, *75*, 035133.
- (20) Mukerjee, S. *Phys. Rev. B* **2005**, *72*, 195109.
- (21) Peterson, M. R.; Mukerjee, S.; Shastry, B. S.; Haerter, J. O. *Phys. Rev. B* **2007**, *76*, 125110.
- (22) Murphy P.; Mukerjee S.; Moore J. 2008, cond-mat/0805.3374 (unpublished).
- (23) Engquist, H.-L.; Anderson, P. W. *Phys. Rev. B* **1981**, *24*, 1151.
- (24) Sivan, U.; Imry, Y. *Phys. Rev. B* **1986**, *33*, 552.
- (25) Butcher, P. N. *J. Phys.: Condens. Matter* **1990**, *2*, 4869.
- (26) Di Ventra M. *Electrical Transport in Nanoscale Systems*; Cambridge University Press: Cambridge, 2008.
- (27) Cahill, D. G.; Ford, W. K.; Goodson, K. E.; Mahan, G. D.; Majumdar, A.; Maris, H. J.; Merlin, R.; Phillpot, S. R. *Appl. Phys. Rev.* **2003**, *93*, 793.
- (28) Bonetto, F.; Lebowitz, J. L.; Rey-Bellet, L. In *Mathematical Physics 2000*; Fokas, A. S., Grigoryan, A., Kibble, T., Zegarlinski, B., Eds.; Imperial College Press: London, 2000; p 128.
- (29) Lindblad, G. *Commun. Math. Phys.* **1976**, *48*, 119.
- (30) Van Kampen, N. G. *Stochastic Processes in Physics and Chemistry*, 2nd ed.; North Holland: Amsterdam, 2001.
- (31) Pershin, Yu. V.; Dubi, Y.; Di Ventra, M. *Phys. Rev. B* **2008**, *78*, 054302.
- (32) A similar form has recently been suggested for spin chains, see: Mejia-Monasterio, C.; Wichterich, H. *Eur. Phys. J.: Spec. Top.* **2008**, *151*, 113.
- (33) Sai, N.; Bushong, N.; Hatcher, R.; Di Ventra, M. *Phys. Rev. B* **2007**, *75*, 115410.
- (34) Note that in a driven system the off-diagonal elements of the DM do not decay at all, and hence it is crucial to calculate them fully, as is done in ref 31. However, in a currentless steady state they vanish identically. A comparison between the approximate method and the full many-body calculation for a small system with similar geometry as discussed here is also presented in ref 31.

- (35) This effect, which is definitely present in real devices, suggests an experimental way to determine the capacitive energy of a nanojunction.
- (36) Pothier, H.; Gu, M. H. *Phys. Rev. Lett.* **1997**, *79*, 3490.
- (37) Surprisingly, these oscillations persist even in the presence of disorder, see: Dubi, Y.; Di Ventra, M. cond-mat/0810.0247.
- (38) Nagy, A.; Parr, R. G.; Liu, S. *Phys. Rev. A* **1996**, *53*, 3117.
- (39) Hartmann, M.; Mahler, G.; Hess, O. *Phys. Rev. Lett.* **2004**, *93*, 080402.
- (40) For a recent review see, e.g.: Michel, M.; Gemmer, J.; Mahler, G. *Int. J. Mod. Phys. B* **2006**, *20*, 4855.
- (41) Gaul, C.; Büttner, H. *Phys. Rev. E* **2007**, *76*, 011111.
- (42) Roy, D. *Phys. Rev. E* **2008**, *77*, 062102.
- (43) Chen, Y.-C.; Zwolak, M.; Di Ventra, M. *Nano Lett.* **2003**, *3*, 1691.
- (44) Huang, Z.; Chen, F.; D'Agosta, R.; Bennett, P. A.; Di Ventra, M.; Tao, N. *Nat. Nanotechnol.* **2007**, *2*, 698.
- (45) (a) Di Ventra, M.; D'Agosta, R. *Phys. Rev. Lett.* **2007**, *98*, 226403.  
(b) D'Agosta, R.; Di Ventra, M. *Phys. Rev. B* **2008**, *78*, 165105.
- (46) Bushong, N.; Di Ventra, M. *J. Phys.: Condens. Matter* **2008**, *20*, 395214.

NL8025407